



Article

# Genetic Analysis and Fine Mapping of *ZmGHT1* Conferring Glufosinate Herbicide Tolerance in Maize (*Zea mays* L.)

Jianxi Bao <sup>1</sup>, Yuexin Gao <sup>1</sup>, Yanan Li <sup>1</sup>, Suowei Wu <sup>1,2</sup> , Jinping Li <sup>2</sup>, Zhenying Dong <sup>1,2,\*</sup>   
and Xiangyuan Wan <sup>1,2,\*</sup>

<sup>1</sup> Zhongzhi International Institute of Agricultural Biosciences, Shunde Graduate School, Research Center of Biology and Agriculture, School of Chemistry and Biological Engineering, University of Science and Technology Beijing, Beijing 100024, China

<sup>2</sup> Beijing Engineering Laboratory of Main Crop Bio-Tech Breeding, Beijing International Science and Technology Cooperation Base of Bio-Tech Breeding, Beijing Solidwill Sci-Tech Co., Ltd., Beijing 100192, China

\* Correspondence: zydong@ustb.edu.cn (Z.D.); wanxiangyuan@ustb.edu.cn (X.W.);  
Tel.: +86-152-1092-0373 (Z.D.); +86-186-0056-1850 (X.W.)

**Abstract:** Weed interference in the crop field is one of the major biotic stresses causing dramatic crop yield losses, and the development of herbicide-resistant crops is critical for weed control in the application of herbicide technologies. To identify herbicide-resistant germplasms, we screened 854 maize inbred lines and 25,620 seedlings by spraying them with 1 g/L glufosinate. One plant (L336R), possibly derived from a natural variation of line L336, was identified to have the potential for glufosinate tolerance. Genetic analysis validated that the glufosinate tolerance of L336R is conferred by a single locus, which was tentatively designated as *ZmGHT1*. By constructing a bi-parental population derived from L336R, and a glufosinate sensitive line L312, *ZmGHT1* was mapped between molecular markers M9 and M10. Interestingly, genomic comparison between the two sequenced reference genomes showed that large scale structural variations (SVs) occurred within the mapped region, resulting in 2.16 Mb in the inbred line B73, and 11.5 kb in CML277, respectively. During the fine mapping process, we did not detect any additional recombinant, even by using more than 9500 F<sub>2</sub> and F<sub>3</sub> plants, suspecting that SVs should also have occurred between L336R and L312 in this region, which inhibited recombination. By evaluating the expression of the genes within the mapped interval and using functional annotation, we predict that the gene *Zm00001eb361930*, encoding an aminotransferase, is the most likely causative gene. After glufosinate treatment, lower levels of ammonia content and a higher activity of glutamine synthetase (GS) in L336R were detected compared with those of L336 and L312, suggesting that the target gene may participate in ammonia elimination involving GS activity. Collectively, our study can provide a material resource for maize herbicide resistant breeding, with the potential to reveal a new mechanism for herbicide resistance.

**Keywords:** maize; herbicide tolerance; fine mapping; structural variation; candidate gene



**Citation:** Bao, J.; Gao, Y.; Li, Y.; Wu, S.; Li, J.; Dong, Z.; Wan, X. Genetic Analysis and Fine Mapping of *ZmGHT1* Conferring Glufosinate Herbicide Tolerance in Maize (*Zea mays* L.). *Int. J. Mol. Sci.* **2022**, *23*, 11481. <https://doi.org/10.3390/ijms231911481>

Academic Editor: Lars Matthias Voll

Received: 21 August 2022

Accepted: 26 September 2022

Published: 29 September 2022

**Publisher's Note:** MDPI stays neutral with regard to jurisdictional claims in published maps and institutional affiliations.



**Copyright:** © 2022 by the authors. Licensee MDPI, Basel, Switzerland. This article is an open access article distributed under the terms and conditions of the Creative Commons Attribution (CC BY) license (<https://creativecommons.org/licenses/by/4.0/>).

## 1. Introduction

Weeds are the major constraint to crop production when compared with other foes, such as pathogens and animal pests, in most cropping systems, producing about 43% of global losses annually [1]. There are more than 35,000 weed species distributed widely around the world, of which about 8000 species are considered troublesome for agriculture [2]. In China, there are more than 1400 weed species having harmful effects for crops [3], and more than 3 million tons of grain losses are caused by weeds each year [4]. While in the United States, maize yield loss due to weed interference is about 50%, causing an estimated annual economic loss of USD 26.7 billion [5].

Because of the high efficacy, low labor requirements, and low cost, herbicides were quickly accepted and adopted by farmers once they were introduced in the late 1940s and early 1950s [6]. Since the introduction of herbicides into China in the late 1950s, they

have currently become the second-most used class of pesticides, following insecticides [7]. However, the intense use of herbicides in the crop field has imposed widespread selection pressure, and herbicide-resistant weeds have quickly evolved, decreasing the number of effective and available herbicides for problematic weeds over time. Currently, 267 (154 dicots and 113 monocots) herbicide resistant weed species have been reported in 72 countries, and weeds have evolved resistance to 21 of the 31 known herbicide sites of action and to 165 different herbicides [8]. For the efficient control of weeds, creating new herbicides that crops, but not weeds, can tolerate, or developing crops that can tolerate herbicides are crucial for weed control and crop production. Due to the long experimental period and high development costs, new herbicides cannot be rapidly commercialized, and there is a risk that the evolutionary rate of herbicide-resistant weeds will possibly exceed the rate of new herbicide discovery [9,10]. Developing herbicide resistant crops that can reduce phytotoxicity after herbicide application is a valuable and practicable alternative for weed management in agriculture.

Depending on the knowledge regarding herbicide-resistant plants, proteins, especially some enzymes, involved in the regulation of key metabolic processes in plant development are the main molecular targets [11,12]. For example, 5-enolpyruvylshikimate-3-phosphate synthase (EPSPS; EC 2.5.1.19) belongs to a kind of amino acid synthase which is a key enzyme in the shikimate pathway for the biosynthesis of aromatic amino acids and phenolics [13,14]. EPSPS is the main target of glyphosate, which is a broad-spectrum, post-emergent herbicide that is most widely used for weed control. Glyphosate can bind to EPSPS irreversibly and compete with the normal substrate phosphoenolpyruvate (PEP) [13,14]. Shikimate will be excessively accumulated once the EPSPS activity is disrupted, and the synthesis of secondary metabolites, including some plant hormones via aromatic amino acids, are also obstructed; these in turn cause disorders in plant growth and ultimately, plant death [13,14]. The mutation of maize EPSPS with T102I and P106S resulted in insensitivity to glyphosate inhibition, but high affinity for PEP has been successfully used commercially for developing glyphosate-resistant maize [15,16]. In addition, investigations of some glyphosate resistant weeds showed that EPSPS gene duplication occurred, and both the transcript and protein accumulation of EPSPS have a linear correlation with the EPSPS genomic copy number, indicating that enough uninhibited EPSPS can also confer glyphosate resistance [11].

Due to the wide application of glyphosate, weed resistance to glyphosate was increasingly reported. A total of 56 glyphosate resistant weed species (from 344 unique cases) have been discovered; in contrast, only 5 glufosinate resistant weed species (from 9 unique cases) have been described [8]. Glufosinate is another non-selective, post-emergent herbicide which is less widely used than glyphosate, and GS (EC 6.3.1.2) is its main target. GS catalyzes the incorporation of ammonia with glutamate to form glutamine, and it is thus essential for plant nitrogen metabolism [17,18]. Glufosinate competes for the glutamate binding site and irreversibly inhibits the activity of GS; the sensitive plants will accumulate excess ammonia quickly after the application of glufosinate, triggering a series of metabolic abnormalities which ultimately induce plant death [17–19]. In higher plants, there are two major GS isoforms, namely cytosolic GS1 and plastidic GS2 [20]. A mutation of D171N in the Italian ryegrass GS2 gene was first reported as correlating with glufosinate resistance [21]. Recently, a novel point mutation (S59G) was identified in the GS1 gene of the *Eleusine indica* glufosinate-resistant population, and the transformed rice with the mutant GS1 gene is resistant to glufosinate [22].

Maize has become the world's second most cultivated crop (FAOSTAT, <https://www.fao.org/faostat>, accessed on 17 February 2022). Weed control via herbicides and the development of new herbicide resistant varieties are both urgently needed for maize production. Herbicide resistant varieties can be obtained by transgenic technologies, or by the mutagenesis of crop genomes and the screening of mutants with enhanced herbicide resistance. There have been 128 recorded transgenic events regarding herbicide-tolerant maize reported in the International Service for the Acquisition of Agri-biotech

Applications (ISAAA, <https://www.isaaa.org/>, accessed on 31 May 2022). However, the public perception and strict regulatory policies developed over centuries gave limited the application of genetically modified (GM) crops [23]. Herbicide-resistance obtained through natural variation or artificial mutagenesis are valuable in breeding herbicide resistant crops, and these methods have been reported in rice and maize [24–27]. In this study, we screened the maize germplasms kept in our institute for glufosinate resistance, and we mapped the *ZmGHT1* conferring glufosinate herbicide tolerance in maize using a segregation population derived from the identified resistant line L336R and a sensitive line L312. The *ZmGHT1* was located in a region of the 2.16 Mb interval of maize chromosome 8 (Chr8), and the candidate gene was predicated, which will provide genetic basis for glufosinate tolerant maize breeding.

## 2. Results

### 2.1. Isolation and Response of L336R to Glufosinate

A total of 854 maize inbred lines with different genetic backgrounds were kept in our laboratory [28]. To isolate the glufosinate tolerant germplasms, 30 seedlings per line were treated with 1 g/L glufosinate, and finally one single plant (designated as L336R), derived from L336, was suspected to possess glufosinate tolerance. L336R was self-pollinated and the derived seedlings were used to evaluate the response to glufosinate. By treating it with 1 g/L glufosinate, progressive injury occurred in L336; the leaves started to turn yellow at 48 h after glufosinate treatment (AGT), and the whole plant dried out and died at 96 h (Figures 1a and S1). However, no visual injury was observed in L336R during the glufosinate treatment (Figures 1a and S1). The above ground biomass measurement showed that the fresh weight of L336 decreased, while that of L336R increased significantly at 96 h AGT (Figure 1b). For the dry weight, L336 showed a slight increase, but a nearly 55% increase occurred in L336R at 96 h AGT (Figure 1b).

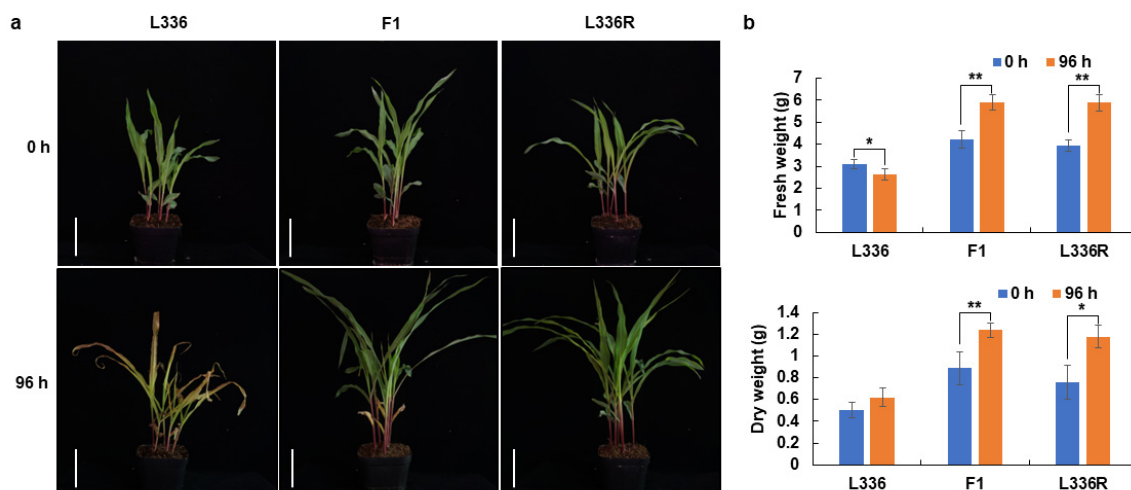


**Figure 1.** Responses to glufosinate among L336, L336R, and the F<sub>1</sub> plants. (a) Visual injury after glufosinate treatment; scale bar = 10 cm; (b) above ground biomass measurement. \* indicates  $p < 0.05$  and \*\* indicates  $p < 0.01$ , respectively.

To further evaluate the glufosinate resistance, different doses of glufosinate were applied to L336R at the three-leaf stage, and the phenotypes were observed at 96 h AGT. The first leaves of the seedlings turned yellow, and seedling growth was obviously inhibited under 5 g/L glufosinate, but the whole plants shrank and began to die after treatment with 8 g/L glufosinate (Figure S2). Such observations indicate that L336R should be tolerant to glufosinate at doses of no more than 5 g/L.

## 2.2. Inheritance of *ZmGHT1*

L336R was first crossed with L336, and it was observed that the F<sub>1</sub> plants behaved in a similar manner to L336R in being resistant to glufosinate after spraying with 1 g/L glufosinate (Figure 1). L336R was then crossed with a glufosinate sensitive line L312, and 192 F<sub>2:3</sub> families from self-pollinated F<sub>2</sub> plants were systematically screened 96 h after glufosinate treatment. A total of 47 and 46 families were identified as homozygously resistant and susceptible to glufosinate, respectively, and 99 families were heterozygous, as both glufosinate susceptible and resistant progenies were obtained (Table 1). The responses of the F<sub>2:3</sub> families to glufosinate were then validated to fit the segregation ratio of 1:2:1, indicating that *ZmGHT1* was segregated from a single dominant locus conferring resistance to glufosinate. The remaining 9500 F<sub>3</sub> seedlings generated from 30 F<sub>2</sub> plants heterozygous for *ZmGHT1* were also examined for glufosinate resistance, and 7057 resistant and 2443 susceptible plants were detected, respectively. Chi-squared testing indicated that the segregation fitted the ratio of 3:1 ( $\chi^2 = 2.596 < \chi^2_{0.05} = 3.841$ ), further suggesting that *ZmGHT1* should be behaved as a single dominant nuclear gene.

**Table 1.** The segregation ratio of F<sub>2:3</sub> families and the chi-squared test.

F <sub>2:3</sub> Family	Observed Frequency	Expected Frequency	$\chi^2$
Homozygous resistance	47	48	0.198
Heterozygous resistance	99	96	
Susceptible	46	48	

$$\chi^2 = 0.198 < \chi^2_{0.05} = 5.991.$$

## 2.3. Genetic Mapping of *ZmGHT1*

F<sub>2</sub> plants derived from the cross of L336R and L312 were used for primary mapping. As a first step, two bulked DNA pools from ten tolerant and ten sensitive F<sub>2</sub> individuals were genotyped using the Maize 60K SNP chip, respectively. Higher polymorphic ratios were detected between 154.38 and 166.67 Mb on Chr8 (Figure 2a); *ZmGHT1* was therefore assigned to Chr8, and SSR markers were developed within this region. In total, 11 polymorphic and co-dominant molecular markers were used for mapping *ZmGHT1* in this study (Table 2).

**Table 2.** The molecular markers used for mapping *ZmGHT1* in this study.

Marker	Forward Primer Sequence	Reverse Primer Sequence
M1	CTGGAAAAGGAGGACTACTG	AAAGCAAGAAGTTGATATAGCC
M2	GGGACGAGTGCCAAATCAG	GGCCTTCGCAAAGAACCAA
M3	CAATCTATCGCTTGACTCATC	GCTACTACTAAGTTGCCCAAAA
M4	CATACTATGTCAAATGCATCC	GAAAACGATGATAAATGGAAGT
M5	TTTCCCACAATACCAACT	GCTAGCTCTTCTGCAATC
M6	AGCCTTGTCTTTGTGGTG	GAACAGTCTGCGACTTGC
M7	CTTCCTTTAACGCCACAA	CGGCACAAGTGTTTCATCA
M8	GGAGATTAAGAGCTGCAA	ATGTTCTGGAAAGTGGTT
M9	TAGACAAGAAACCAACAT	CAAAGGTAAGGTGAGAC
M10	CCAACACGTGGCAGGCAG	CGCCGAGTCACCAATCCAC
M11	TATGAGTAAGTAGCGTGAAGCA	CCTATCTATTGGAAGCCTATGA

Using molecular markers of M1 to M4 and 318 F<sub>2</sub> plants with known phenotypes, *ZmGHT1* was primarily located in a 4.21 Mb region between markers M2 and M3 (Figure 2b). To further narrow the mapped region of *ZmGHT1*, 7 additional molecular markers (M5 to M11) were used, and although a large population possessing up to 9,500 F<sub>3</sub> plants were examined, only 1 resistant plant (F<sub>3</sub>-106) and 1 susceptible plant (F<sub>3</sub>-78) were detected with recombinations between the markers M9 and M10, which cover a 2.16 Mb region, respectively (Figure 2c,d). These key recombinants indicate that *ZmGHT1* is located in a

physical region of 160.12–162.28 Mb in Chr8, and the recombination rate in this interval is fairly low.

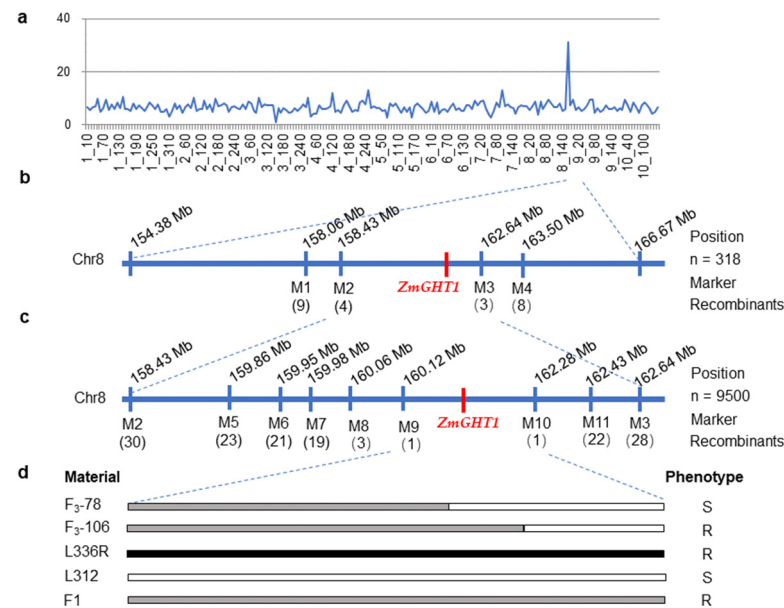


**Figure 2.** Fine mapping of *ZmGHT1*. (a) Polymorphic ratios between tolerant and sensitive DNA pools detected by the Maize 60K SNP chip; (b) primary mapping of *ZmGHT1*, and the *ZmGHT1* region was delimited to a 4.21 Mb interval between M2 and M3 in Chr8; (c) fine mapping of *ZmGHT1*, and the *ZmGHT1* was mapped between M9 and M10; (d) illustration of the key recombinants and phenotype determination. Black bars represent chromosomal fragments derived from L336R, white bars represent the fragments derived from L312, and gray bars indicate the heterozygous regions.

To investigate the mechanism of the low recombination rate in the mapped region, four relatively long fragments (1.2–1.5 kb) were amplified from the M7 to M10 sites (Fragment 1 to Fragment 4) using L336R and L312 as templates, respectively (Table S1). Sequence comparisons were performed using the BLAST algorithm against MaizeGDB, and the results showed that the SNP and indel patterns of the PCR products of L336R are more similar to the inbred line B73, while the patterns in L312 are more similar to another sequenced inbred line, CML277 (Figures S3–S6). Further, we found that the sequence identity between L336R and B73 is 100%, while the sequence identity between L336R and CML277 is 97.1% (Table S2). In contrast, the sequence identity between L312 and CML277 is 99.6%, while the sequence identity between L312 and B73 is 97.4% (Table S2). Thus, we suspect that the sequence composition in the mapped region of L336R should be more similar to B73, while L312 is possibly similar to CML277. Interestingly, only 11.5 kb sequences exist between the M9 and M10 intervals in CML277 genome. We then retrieved the sequences between M8 and M10, where a low recombination rate was detected from B73 (2.22 Mb) and CML277 (51.73 kb), respectively. The genomic structure comparison showed that both sequence rearrangement and insertion/deletion exist between B73 and CML277 (Figure 3a). We suspect that these types of structural variations (SVs) may also exist in this region between L336R and L312, inhibiting the recombination in the *ZmGHT1* locus. We further investigated the sequence characteristics and found that relatively higher densities of transposable elements (TEs) presented in this region of the B73 genome (Figure 3b). As TE insertional polymorphisms were widely observed in the maize population [29,30], we suspect that TE insertion or deletion should be one of the reasons for the sizable SVs in the *ZmGHT1* locus.

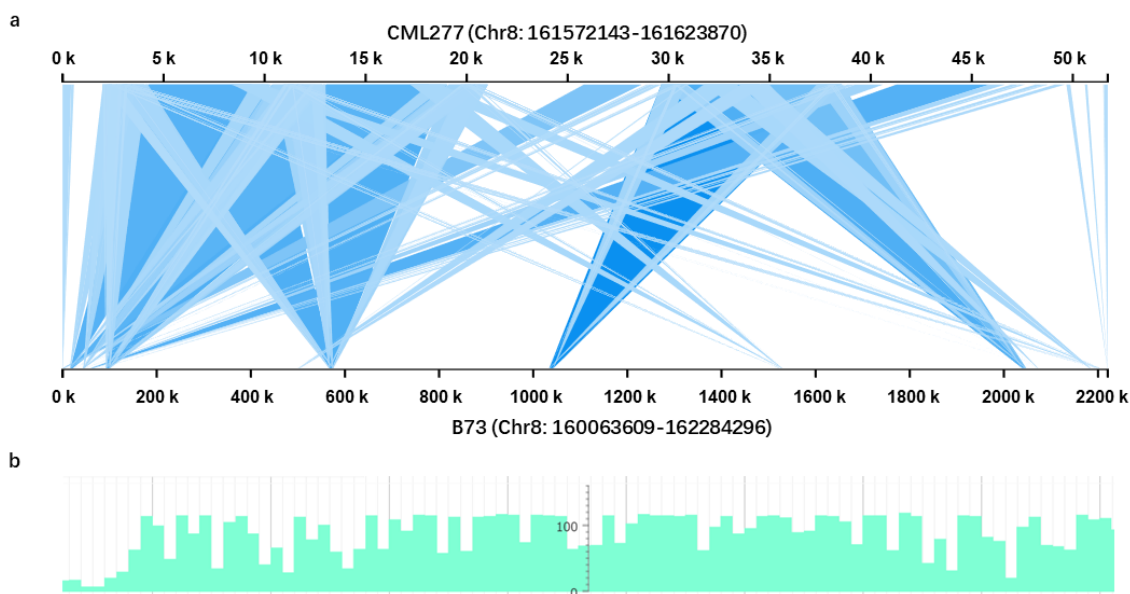


**Figure 3.** Sequence comparison between B73 and CML277 in the *ZmGHT1* locus. (a) Illustration of the SVs between B73 and CML277 in the *ZmGHT1* locus. (b) Distribution of the TEs in the *ZmGHT1* locus based on B73 genome sequence information.

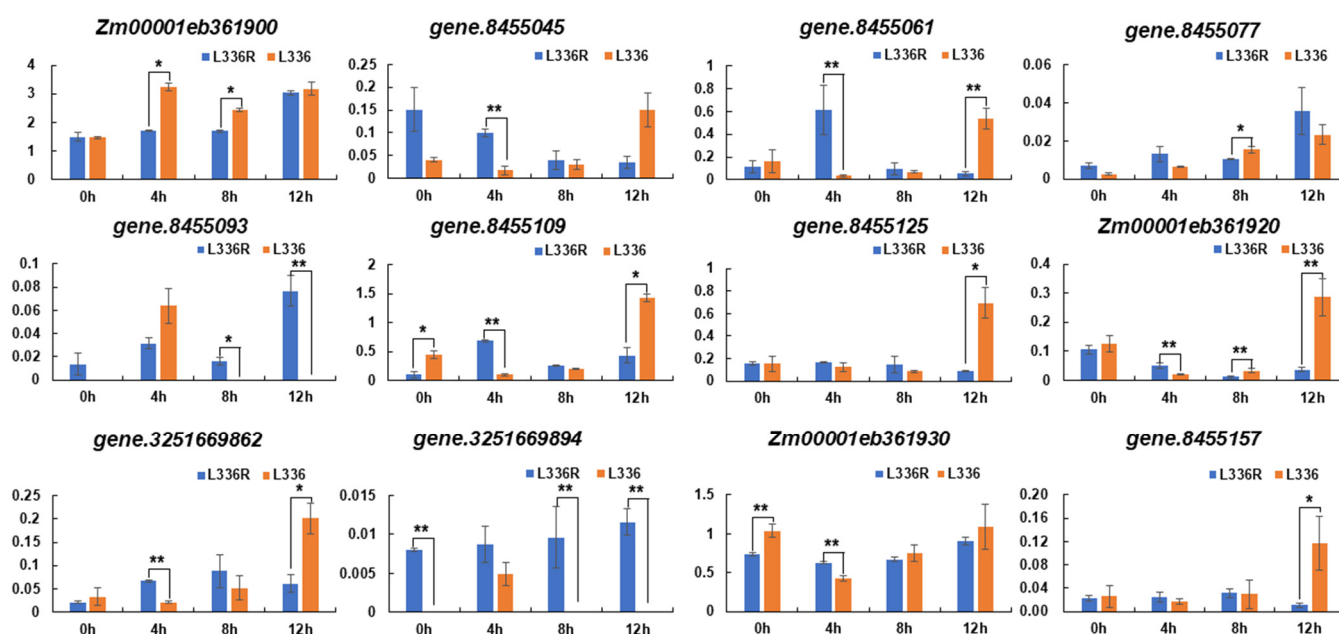
#### 2.4. Candidate Gene Prediction, Functional Annotation, and Expression Analysis

According to the annotation of the B73 reference genome in MaizeGDB, three genes, namely *Zm00001eb361900*, *Zm00001eb361920* and *Zm00001eb361930* have been predicted between M9 and M10 (Table 3). However, according to the NCBI Gnomon Gene Models [31], ten more genes were predicted (Table 3). All the thirteen genes were first functionally annotated by sequence similarity searches against GenBank. Nine were predicted as the protein coding genes and eight genes have functional annotations, among which *Zm00001eb361930* and *gene.3251669926* possibly encode class III aminotransferases, and *gene.8455157* encodes a cationic amino acid transporter (Table 3).

We then examined the transcription patterns of the thirteen genes in response to glufosinate treatment in L336 and L336R by quantitative real time-PCR (qRT-PCR) using gene specific primers (Table S3). Except for *gene.3251669926*, all the other twelve candidate genes were detected for transcript accumulation at different time points, and *Zm00001eb361900*, *gene.8455061*, *gene.8455109*, *gene.8455125*, and *Zm00001eb361930* were relatively highly transcribed when compared to the remaining numbers (Figure 4). During the treatment with glufosinate, the temporal transcription patterns of specific genes changed and diverged significantly between L336 and L336R (Figure 4). For example, transcript levels of *Zm00001eb361900* increase after glufosinate treatment in both lines, but the transcript levels were significantly higher in L336 than those in L336R at 4 h and 8 h AGT, respectively (Figure 4). For *Zm00001eb361930*, which possibly participates in catalyzing amino groups, according to functional annotation, the transcript level was relatively higher before glufosinate treatment (0 h) in L336; however, the transcript level of L336R is statistically significantly higher than that of L336 at 4 h AGT ( $p < 0.01$ ) (Figure 4). Although accumulation of the transcripts increased temporally, no significant differences were detected for *Zm00001eb361930* between L336 and L336R (Figure 4).

**Table 3.** Predicated genes in the *ZmGHT1* locus, their chromosomal location, and functional annotations.

Gene ID	Start	End	Strand	Functional Annotation
<i>Zm00001eb361900</i>	160124107	160128959	+	Epstein–Barr nuclear antigen
<i>gene.8455045</i>	160775402	160775752	–	No significant similarity
<i>gene.8455061</i>	160782742	160783140	–	No significant similarity
<i>gene.8455077</i>	160783139	160783441	+	No significant similarity
<i>gene.8455093</i>	161011640	161011329	+	No significant similarity
<i>gene.8455109</i>	161124578	161128321	+	Uncharacterized protein
<i>gene.8455125</i>	161128385	161129846	–	Embryogenesis transmembrane protein-like
<i>Zm00001eb361920</i>	161130057	161130464	–	Embryogenesis transmembrane protein-like
<i>gene.3251669862</i>	161493564	161495449	–	Retrovirus-related Pol polyprotein LINE-1
<i>gene.3251669894</i>	161495561	161495668	–	SH3 domain-containing protein 2
<i>gene.3251669926</i>	162029341	162030174	–	class III aminotransferase
<i>Zm00001eb361930</i>	162030458	162031088	–	class III aminotransferase
<i>gene.8455157</i>	162031992	162033874	–	Cationic amino acid transporter 1

**Figure 4.** Transcript level evaluation of the candidate genes in the *ZmGHT1* locus. *Gene.3251669926* was excluded due to no transcript accumulation at any time points; \* indicates  $p < 0.05$  and \*\* indicates  $p < 0.01$ , respectively.

### 2.5. GS Activity Levels and Ammonia Content Determination during Glufosinate Treatment

To evaluate the physiological response to glufosinate in maize, two sensitive lines L312 and L336, as well as the resistant line L336R, were treated with 1g/L glufosinate. Compared with mock treatment, GS activities of the crude extracts of L312 and L336 were rapidly and significantly decreased after glufosinate application, more than 50% reductions were observed from 2 h AGT for the both sensitive lines, and GS activity remained at roughly the same low levels during the treatment (Figure 5a). However, GS activity in L336R was less sensitive to glufosinate; the statistically significant reduction was detected until at 8 h AGT, and GS activity was slightly restored thereafter (Figure 5a).

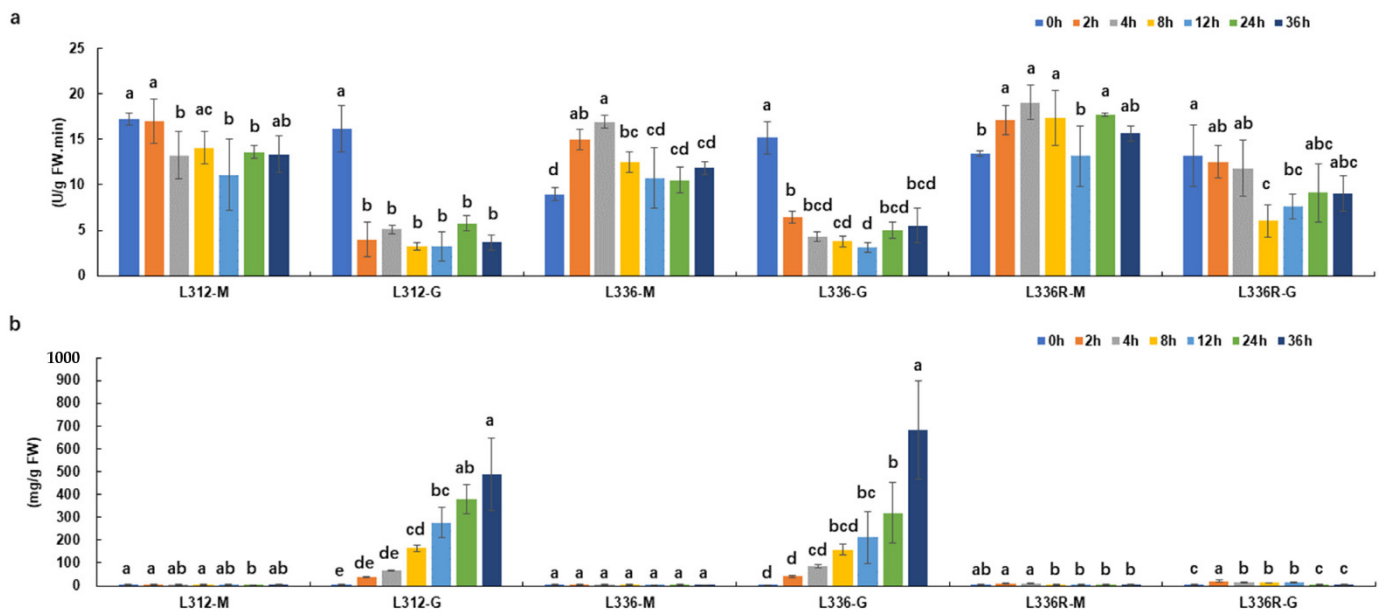


**Figure 5.** GS activity levels (a) and ammonia content (b) determination during glufosinate treatment. Different letters above each histogram bar indicate significant differences ( $p < 0.05$ ). M: mock; G: glufosinate.

As for ammonia, which is substrate of the reaction catalyzed by GS, no more than 10 mg ammonia per  $\text{kg}^{-1}$  fresh weight leaves were detected from untreated or water-treated plants (Figure 5b). After glufosinate treatment, the highest level of ammonia in L336R was observed at 2 h AGT, and 21.6 mg ammonia per g fresh weight ( $\text{g}^{-1}$  FW) leaves were accumulated, but the levels were then gradually restored to their original status over time (Figure 5b). For L312 and L336, rapid and significant increase in ammonia levels was observed after glufosinate treatment, up to 682.4 mg/  $\text{g}^{-1}$  FW leaves of ammonia was detected at 36 h AGT (Figure 5b). The above data indicate that the application of glufosinate does not significantly induce in vivo ammonia accumulation in L336R.

### 2.6. Detection Efficiency Test of M9 and M10 for Identifying Functional Allele of *ZmGHT1*

A  $\text{BC}_2\text{F}_2$  population including 360 seedlings, using L312 as the recurrent parent, was generated. By genotyping with M9 or M10, the same 264 seedlings were found to contain the *ZmGHT1* functional allele (Figure 6). All the 360 seedlings were then treated with 1 g/L glufosinate, and the 264 seedlings with the *ZmGHT1* functional allele survived, while the remaining 96 seedlings gradually died, indicating that M9 and M10 have high efficiencies for selecting the *ZmGHT1* functional allele.

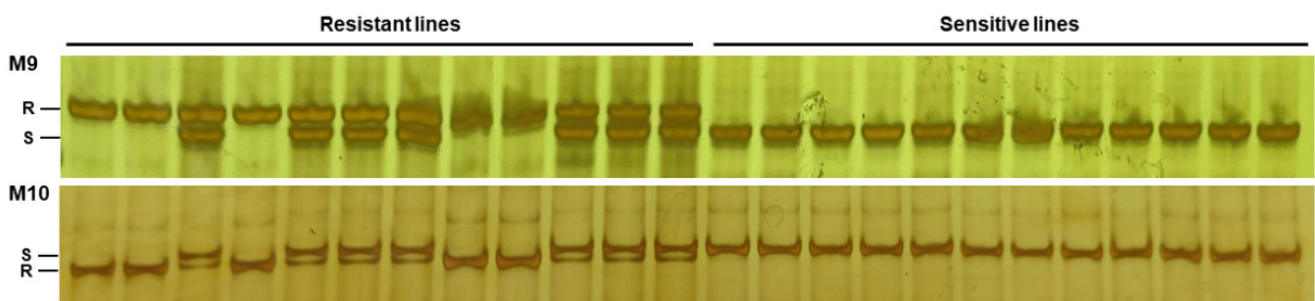


**Figure 6.** Selection efficiency validation of M9 and M10 for the *ZmGHT1* functional allele. A total of 12 resistant and sensitive seedlings were randomly selected, respectively. R: resistant allele; S: sensitive allele.

### 3. Discussion

Herbicides have been used as a major tool for controlling weeds in the crop fields for more than a half century [6,7]. However, the emergence of weeds resistant to widely used herbicides brings new challenges for both crop growers and scientific researchers. Considering the lower appearance rate of glufosinate resistant weeds and its potential use as an alternative herbicide to glyphosate [8,18], we screened the in-house retained maize germplasms and identified a line called L336R, which is tolerant to glufosinate (Figure 1). Further dose–response studies showed that L336R can tolerate more than two times the recommended concentration of glufosinate for weed control (Figure S2), indicating that L336R can be used as germplasm resource for breeding glufosinate tolerant maize. Genetic analysis showed that glufosinate resistance of L336R was conferred by a single locus in maize Chr8, which was tentatively named *ZmGHT1* (Table 1). In the maize genome, five genes for GS1 subunits (Gln1-1 to Gln1-5) and one gene for GS2 were annotated [32,33]. We checked their chromosomal location and found that they are located on chromosomes 1, 4, 5, 9, and 10, respectively, indicating that *ZmGHT1* should not be derived from the GS gene variation, but possibly from an uncharacterized molecular target of glufosinate.

To fine map *ZmGHT1*, a biparental population was constructed. The mapped region is located in the distal region (160.12–162.28 Mb) of Chr8, which possesses a total length of 182.41 Mb sequences (Figure 2). Although a high recombination rate tends to occur in this type of subtelomeric region [34,35], extraordinarily few recombinants were detected, even using 9500 F<sub>3</sub> seedlings, indicating that recombination is inhibited in the *ZmGHT1* locus. Recently, fine mapping and candidate gene identification of *Ga1* locus which, have been pursued for many years, were successfully conducted, and genomic structure analysis showed that few syntenic blocks exist between the *Ga1-S* and *ga1* genomes, which is the main reason why so few recombinant individuals were detected [36]. We therefore suspect that vast SVs between L336R and L312 in the *ZmGHT1* locus may also exist. Although the genomic sequence information is not available for L336R and L312, these two inbred lines were predicted to resemble B73 and CML277, respectively, based on sequence comparison (Figures S3–S6). Only 11.5 kb sequences were retrieved between markers M9 and M10, with a high density of TEs inserted in the non-syntenic regions of CML277 (Figure 3). This may explain the reason why so few recombinants were detected for fine mapping *ZmGHT1*. However, we cannot rule out the possible participation of other mechanisms, as studies regarding *Brassica* genomes have shown that recombination was precluded in hypermethylated regions [37].

Although phenomena of herbicide resistance have been discovered for decades, and 26 molecular target sites of herbicides have been classified by the Resistance Action Committee (<https://hracglobal.com/tools/hrac-mode-of-action-classification-2022-map>, accessed on 1 January 2022), new molecular targets and variations involving herbicide resistance are consistently and continuously being discovered [38–43]. In this study, eight genes located in the mapped interval were functionally annotated, among which *Zm00001eb361930* and gene.8455157, possibly encoding a class III aminotransferase and a cationic amino acid transporter, respectively, were detected for expression in the leaves during glufosinate treatment (Figure 4; Table 2). At least three types of amino acid metabolic enzymes, including EPSPSs, GSs, and the acetolactate synthases (ALSs; EC 2.2.1.6), which are crucial in the synthesis of branched-chain amino acids, have been validated as targets of different herbicides [14,17,18,44]. Specific point mutation of these enzymes endowed herbicide resistance in plants [14,18,44]. Some transferases including glutathione S-transferases (GSTs; EC 2.5.1.18) and glucosyltransferases (GTs; EC 2.4), as well as ATP-binding cassette (ABC) transporters have also been reported to be involved in detoxifying herbicides [11,41]. The above information indicates that both *Zm00001eb361930* and gene.8455157 may participate in herbicide reaction, and they are possible candidate genes for *ZmGHT1*. While assessing the expression patterns during glufosinate treatment (Figure 4), we considered *Zm00001eb361930* as the most possible candidate gene. As prominent accumulation of ammonia and a reduction in GS activity were also observed (Figure 5), indicating that the

candidate gene may participate in ammonia metabolism. We found that the expression pattern of *Zm00001eb361930* is highly correlated with the fluctuation of GS activity in the resistant line L336R, that is, the reduction and restoration during glufosinate treatment (Figures 4 and 5). It would thus be interesting to study the relationship between the candidate gene and ammonia catabolism and GS activity in the future.

Molecular markers M9 and M10 were used to test the selection efficiency of the *ZmGHT1* functional allele in a BC<sub>2</sub>F<sub>2</sub> population (Figure 6). About three-fourths of the seedlings were detected to contain the *ZmGHT1* functional allele, and all of them survived after glufosinate treatment, while the remaining seedlings died. Therefore, M9 and M10 are efficient in tagging *ZmGHT1*, which should accelerate the use of this important gene in marker-assisted selection for breeding glufosinate resistant cultivars in maize.

In summary, we isolated a glufosinate resistant maize line L336R derived from natural variation, and the locus *ZmGHT1* conferring glufosinate herbicide tolerance in maize was mapped between M9 and M10 in Chr8, spanning an interval of 2.16 Mb using B73 as a reference. However, only 11.5 kb sequences were discovered in the orthologous region of CML277. Genomic structure analysis showed that SVs, including sequence rearrangement and TE insertion/deletion, are the main mechanisms for the polymorphisms. *Zm00001eb361930* located in the mapped interval is the most likely candidate gene, as determined by combining functional annotation and gene expression analysis. Our study will provide a material resource for maize herbicide-resistant breeding, with the potential to reveal a new mechanism for herbicide resistance.

## 4. Materials and Methods

### 4.1. Plant Materials and Phenotyping

In 2019, 854 maize inbred lines with 30 repetitions per line were planted in an experimental station of the University of Science and Technology Beijing in Pinggu, Beijing. At the three-leaf stage, all the 25,620 plants were screened by spraying them with 1 g/L glufosinate (Tianjin Huayu pesticide, Tianjin, China). A dose of 1 g/L was recommended by the producer for controlling normal weeds, while for perennial and resistant weeds, 2 g/L was recommended. One single plant with the glufosinate resistance potential was identified from maize inbred line L336, and it was tentatively nominated as L336R. L336R was then self-pollinated for propagation and crossed with L336 and another inbred line L312 as male parental line, respectively.

For investigating the response of L336R to glufosinate treatment and genetic inheritance, seeds of L336R, L336, and the F<sub>1</sub> hybrids were germinated and grown in a greenhouse setting in a 16/8 h light/dark photoperiod with 28/22 °C temperatures. The three types of plants were treated with 1 g/L glufosinate at the three-leaf stage. To compare the fresh and dry weights of the above-ground parts, five seedlings per material were measured. Different concentrations of glufosinate ammonium (0, 1, 2, 3, 4, 5, and 8 g/L) were further used for testing the herbicide tolerance of L336R.

### 4.2. Genetic Mapping Population Construction and Fine Mapping of *ZmGHT1*

By crossing L336R with a glufosinate sensitive line L312 and self-pollinating the F<sub>1</sub> plants, 318 F<sub>2</sub> progenies were used for primary mapping. As a first step, ten F<sub>2</sub> individuals of each phenotype were randomly selected for constructing a glufosinate tolerant and a sensitive bulked DNA pool, respectively. SNP polymorphism analysis was performed by using the Maize 60K SNP chip [45]. Genotyping using the Affymetrix GeneTitan platform (Thermo Fisher Scientific Affymetrix, Santa Clara, CA, USA) was performed, and the polymorphic ratios between the two bulked DNA pools were calculated in each of the 10-Mb sliding windows along the maize 10 chromosomes, and the successive region with a high polymorphic ratio was considered as the candidate region for *ZmGHT1*.

A total of 192 F<sub>2</sub> plants were randomly selected and self-pollinated to generate F<sub>2:3</sub> families used for testing the segregation ratio of glufosinate tolerance; 9500 F<sub>3</sub> seedlings generated from 30 F<sub>2</sub> plants heterozygous for *ZmGHT1* were used for fine mapping.

To test the detection efficiency of the flanking linked markers for identifying the functional allele of *ZmGHT1*, a BC<sub>2</sub>F<sub>2</sub> population including 360 seedlings was constructed using sensitive line L312 as the recurrent parent and L336R as the pollen donor.

#### 4.3. Molecular Marker Development

The Maize 60K SNP chip assay showed that the highest polymorphic ratio occurred in the region between 154.38 Mb and 166.67 Mb in Chr8, according to the information of the B73 reference genome (AGPv5). Thus, the sequences between this interval were downloaded from MaizeGDB (<https://www.maizegdb.org/>, accessed on 3 August 2022), and the simple sequence repeats (SSRs) were searched using the SSR Locator program [46]; the primer pairs flanking each SSR site were designed by software Primer Premier 5.0, polymorphisms for all the molecular markers were first tested using L336R and L312 as samples, and only the co-dominant markers were retained and used for subsequent analysis.

#### 4.4. Extraction of Genomic DNA and PCR Conditions

Genomic DNA was extracted from the three-leaf stage of relevant maize samples using a modified method [47]; PCR was conducted using 2× EasyTaqPCR SuperMix according to the manufacturer's instructions (TransGen, Beijing, China). The main cycling conditions for PCR included a pre-denaturation step at 94 °C for 3 min, 35 cycles of denaturation at 94 °C for 30 s, primer annealing at 50–60 °C (adjusted depending on specific primer pairs) for 30 s, and extension at 72 °C for 45 s; a final extension was set at 72 °C for 5 min. The primer sequences for molecular markers are listed in Table 2. The primer pairs for cloning the four fragments from the M7 to M10 regions (Fragment 1 to Fragment 4), as well as the positional information based on the B73 genome, are provided in Table S1.

#### 4.5. Sequence Analysis

A sequence similarity search was performed using the BLAST program [48]. Sequence alignment was performed using Clustal W [49]; sequence identity was analyzed by Mat-GAT2.01 [50], and further analyzed and visualized by DNAMAN version 6.0 (Lynnon Biosoft, Quebec City, QC, Canada). For visualization of the SVs of molecular markers M8 to M10 between B73 and CML277, a web-based BLAST results visualizer Kablammow was used [51].

#### 4.6. RNA Extraction and Gene Expression Analysis

Seeds of L336 and L336R were sowed in plastic pots and treated with 1 g/L glufosinate at the three-leaf stage. The third leaves were harvested at 0 h, 4 h, 8 h, and 12 h time points, and total RNA was extracted using Trizol reagent according to manufacturer's protocol (Invitrogen, Waltham, MA, USA). The quality of the RNA was evaluated spectrophotometrically using NanoDrop 2000 (Thermo Scientific, Waltham, MA, USA). The reverse transcription (RT) reaction was performed using a 5× All-in-One RT MasterMix (Applied Biological Materials, Richmond, BC, Canada) in a 10 µL reaction with 500 ng of RNA as a template, following the manufacturer's instructions. qRT-PCR analyses of the candidate genes were conducted on the QuantStudio 5 Real-Time PCR System (ABI, Carlsbad, CA, USA) using TB Green™ Premix Ex Taq™ (TaKaRa, Kyoto, Japan). *ZmActin1* was chosen and used as the internal control [52]. The data were analyzed by the  $2^{-\Delta\Delta C_t}$  method.

#### 4.7. Ammonia Accumulation Measurement

At the three-leaf stage, seedlings of L336R and L336 were sprayed with 1g/L glufosinate and distilled water (mock treatment), respectively, in a greenhouse. For ammonia extraction, the third leaves from individual plants were collected at 0, 2, 4, 8, 12, 24, and 36 h after treatment. A total of 500 mg of fresh tissues from five seedlings per sample were collected, quickly frozen in liquid nitrogen, and stored at −80 °C in an ultra-freezer until analysis. The ammonia content per g of fresh weight (mg/g<sup>-1</sup> FW) leaves was determined by spectrophotometry, according to methods of Weatherburn [53], using a UV-visible

spectrophotometer (Thermo Electron, Waltham, MA, USA) at a 625 nm wavelength. The assessment was conducted in triplicate.

#### 4.8. GS Activity Determination

GS was extracted and measured according to the method of Ding et al. [54], using a Glutamine Synthetase (GS) Assay Kit (Solarbio, Beijing, China). In brief, 500 mg of fresh tissues from five seedlings per sample were collected, ground thoroughly in liquid nitrogen, and then diluted in 1 mL of extraction buffer. After centrifuging at  $5000\times g$  for 10 min, the supernatant was collected for activity measurement. The absorbance at 540 nm was recorded for the calculation of GS activity. The assessment was conducted in triplicate. The change in the absorbance value of 0.005 at 540 nm per minute  $g^{-1}$  FW leaves in the reaction system was defined as one enzyme activity unit.

#### 4.9. Statistical Analysis

Data from this study were reported as mean  $\pm$  standard deviation (SD). Results were subjected to analysis of variance (ANOVA) using SPSS 25.0 software (IBM SPSS Statistics for Windows, Armonk, NY, USA). Significant differences between means were assessed by Fisher's protected least significance difference (LSD).

**Supplementary Materials:** The following supporting information can be downloaded at: <https://www.mdpi.com/article/10.3390/ijms231911481/s1>.

**Author Contributions:** Conceptualization, X.W. and Z.D.; methodology, J.B.; validation, S.W., Z.D., and X.W.; formal analysis, J.B., Y.G., and Y.L.; investigation, J.B.; resources and data curation, X.W. and Z.D.; writing—original draft preparation, Z.D.; writing—review and editing, X.W. and Z.D.; visualization, J.B.; supervision, J.L.; project administration, X.W. and Z.D.; funding acquisition, S.W., Z.D., and X.W. All authors have read and agreed to the published version of the manuscript.

**Funding:** This research was funded by the National Key R&D Program of China (2018YFD1000700, 2021YFF1000302, 2021YFD1200700) and the Fundamental Research Funds for the Central Universities of China (06500136).

**Institutional Review Board Statement:** Not applicable.

**Informed Consent Statement:** Not applicable.

**Data Availability Statement:** The data is contained within the article or Supplementary Materials.

**Conflicts of Interest:** The authors declare no conflict of interest. Beijing Solidwill Sci-Tech Co., Ltd. operates the Beijing Engineering Laboratory and Beijing International Science and Technology Cooperation Base, which provided the research platform, instruments, and funds for this study; therefore, the company is one of the disclosed funders of this paper.

## References

1. Oerke, E.C. Crop losses to pests. *J. Agri. Sci.* **2006**, *144*, 31–43. [[CrossRef](#)]
2. Holm, L.G.; Plucknett, D.L.; Pancho, J.V.; Herberger, J.P. *The World Worst Weeds. Distribution and Biology*; University Press of Hawaii: Honolulu, HI, USA, 1977.
3. Li, Y.H.; Yang, R.J.; Yang, B.Z.; Wu, W.C.; Zhang, L.Y.; Qiang, S.; Islam, F.; Yang, C.; Chen, X.; Zhou, W. *Weed Flora in China*; China Agriculture Press: Beijing, China, 1998.
4. Zhu, J.; Wang, J.; Ditommaso, A.; Zhang, C.; Zheng, G.; Liang, W.; Islam, F.; Yang, C.; Chen, X.; Zhou, W. Weed research status, challenges, and opportunities in china. *Crop Prot.* **2020**, *134*, 104449. [[CrossRef](#)]
5. Soltani, N.; Dille, J.A.; Burke, I.C.; Everman, W.J.; Van Gessel, M.J.; Davis, V.M.; Sikkema, P.H. Potential corn yield losses from weeds in North America. *Weed Technol.* **2016**, *30*, 979–984. [[CrossRef](#)]
6. Clay, S.A. Near term challenges for global agriculture-herbicide resistant weeds. *Agron J.* **2021**, *113*, 4463–4472. [[CrossRef](#)]
7. Liu, X.; Merchant, A.; Xiang, S.; Zong, T.; Zhou, X.; Bai, L. Managing herbicide resistance in China. *Weed Sci.* **2021**, *69*, 4–17. [[CrossRef](#)]
8. Heap, I. The International Herbicide-Resistant Weed Database. Available online: [www.weedscience.org](http://www.weedscience.org) (accessed on 12 August 2022).
9. Green, J.M. Current state of herbicides in herbicide-resistant crops. *Pest Manag. Sci.* **2014**, *70*, 1351–1357. [[CrossRef](#)]
10. Gaines, T.A.; Busi, R.; Küpper, A. Can new herbicide discovery allow weed management to outpace resistance evolution? *Pest Manag. Sci.* **2021**, *77*, 3036–3041. [[CrossRef](#)]

11. Gaines, T.A.; Duke, S.O.; Morran, S.; Rigon, C.A.G.; Tranel, P.J.; Küpper, A.; Dayan, F.E. Mechanisms of evolved herbicide resistance. *J. Biol. Chem.* **2020**, *295*, 10307–10330. [[CrossRef](#)]
12. Hall, C.J.; Mackie, E.R.; Gendall, A.R.; Perugini, M.A.; Soares da Costa, T.P. Review: Amino acid biosynthesis as a target for herbicide development. *Pest. Manag. Sci.* **2020**, *76*, 3896–3904. [[CrossRef](#)]
13. Dill, G.M. Glyphosate-resistant crops: History, status and future, *Pest Manag. Sci.* **2005**, *6*, 1219–1224.
14. Sammons, D.R.; Gaines, T.A. Glyphosate resistance: State of knowledge. *Pest Manag. Sci.* **2014**, *70*, 1367–1377. [[CrossRef](#)] [[PubMed](#)]
15. Sidhu, R.S.; Hammond, B.G.; Fuchs, R.L.; Mutz, J.N.; Holden, L.R.; George, B.; Olson, T. Glyphosate-tolerant corn: The composition and feeding value of grain from glyphosate-tolerant corn is equivalent to that of conventional corn (*Zea mays* L.). *J. Agric. Food Chem.* **2000**, *48*, 2305–2312. [[CrossRef](#)] [[PubMed](#)]
16. Funke, T.; Yang, Y.; Han, H.; Healy-Fried, M.; Olesen, S.; Becker, A.; Schönbrunn, E. Structural basis of glyphosate resistance resulting from the double mutation Thr<sup>97</sup> → Ile and Pro<sup>101</sup> → Ser in 5-enolpyruvylshikimate-3-phosphate synthase from *Escherichia coli*. *J. Biol. Chem.* **2009**, *284*, 9854–9860. [[CrossRef](#)] [[PubMed](#)]
17. Kishore, G.M.; Shah, D.M. Amino acid biosynthesis inhibitors as herbicides. *Annu. Rev. Biochem.* **1988**, *57*, 627–663. [[CrossRef](#)] [[PubMed](#)]
18. Takano, H.K.; Dayan, F.E. Glufosinate-ammonium: A review of the current state of knowledge. *Pest Manag. Sci.* **2020**, *76*, 3911–3925. [[CrossRef](#)]
19. Hess, F.D. Light-dependent herbicides: An overview. *Weed Sci.* **2000**, *48*, 160–170. [[CrossRef](#)]
20. Unno, H.; Uchida, T.; Sugawara, H.; Kurisu, G.; Sugiyama, T.; Yamaya, T.; Sakakibara, H.; Hase, T.; Kusunoki, M. Atomic structure of plant glutamine synthetase: A key enzyme for plant productivity. *J. Biol. Chem.* **2006**, *281*, 29287–29296. [[CrossRef](#)]
21. Avila-Garcia, W.V.; Sanchez-Olguin, E.; Hulting, A.G.; Mallory-Smith, C. Target-site mutation associated with glufosinate resistance in Italian ryegrass (*Lolium perenne* L. ssp. *multiflorum*). *Pest Manag. Sci.* **2012**, *68*, 1248–1254. [[CrossRef](#)]
22. Zhang, C.; Yu, Q.; Han, H.; Yu, C.; Nyporko, A.; Tian, X.; Beckie, H.; Powles, S. A naturally evolved mutation (Ser59Gly) in glutamine synthetase confers glufosinate resistance in plants. *J. Exp. Bot.* **2022**, *73*, 2251–2262. [[CrossRef](#)]
23. Sharma, P.; Singh, S.P.; Iqbal, H.M.N.; Parra-Saldivar, R.; Varjani, S.; Tong, Y.W. Genetic modifications associated with sustainability aspects for sustainable developments. *Bioengineered* **2022**, *13*, 9508–9520. [[CrossRef](#)]
24. Kuang, Y.; Li, S.; Ren, B.; Yan, F.; Spetz, C.; Li, X.; Zhou, X.; Zhou, H. Base-editing-mediated artificial evolution of *OsALS1* in planta to develop novel herbicide-tolerant rice germplasm. *Mol. Plant* **2020**, *13*, 565–572. [[CrossRef](#)] [[PubMed](#)]
25. Maeda, H.; Murata, K.; Sakuma, N.; Takei, S.; Yamazaki, A.; Karim, M.R.; Kawata, M.; Hirose, S.; Kawagishi-Kobayashi, M.; Taniguchi, Y.; et al. A rice gene that confers broad-spectrum resistance to  $\beta$ -triketone herbicides. *Science* **2019**, *365*, 393–396. [[CrossRef](#)] [[PubMed](#)]
26. Sun, Y.; Zhang, X.; Wu, C.; He, Y.; Ma, Y.; Hou, H.; Guo, X.; Du, W.; Zhao, Y.; Xia, L. Engineering herbicide-resistant rice plants through CRISPR/Cas9-mediated homologous recombination of acetolactate synthase. *Mol. Plant* **2016**, *9*, 628–631. [[CrossRef](#)] [[PubMed](#)]
27. Jiang, Y.Y.; Chai, Y.P.; Lu, M.H.; Han, X.L.; Lin, Q.; Zhang, Y.; Zhang, Q.; Zhou, Y.; Wang, X.C.; Gao, C.; et al. Prime editing efficiently generates W542L and S621I double mutations in two *ALS* genes in maize. *Genome Biol.* **2020**, *21*, 257. [[CrossRef](#)]
28. Qin, W.; Bao, J.; Wang, Y.; Ma, Y.; Long, Y.; Li, J.; Dong, Z.; Wan, X. Genome-wide association study of leaf angle traits and mining of elite alleles from the major loci in maize. *Acta Agron. Sin.* **2022**, *48*, 2691–2705. [[CrossRef](#)]
29. Anderson, S.N.; Stitzer, M.C.; Brohammer, A.B.; Zhou, P.; Noshay, J.M.; O'Connor, C.H.; Hirsch, C.D.; Ross-Ibarra, J.; Hirsch, C.N.; Springer, N.M. Transposable elements contribute to dynamic genome content in maize. *Plant J.* **2019**, *100*, 1052–1065. [[CrossRef](#)]
30. Qiu, Y.; O'Connor, C.H.; Della Coletta, R.; Renk, J.S.; Monnahan, P.J.; Noshay, J.M.; Liang, Z.; Gilbert, A.; Anderson, S.N.; McGaugh, S.E.; et al. Whole-genome variation of transposable element insertions in a maize diversity panel. *G3 (Bethesda)* **2021**, *11*, jkab238. [[CrossRef](#)]
31. Souvorov, A.; Kapustin, Y.; Kiryutin, B.; Chetvernin, V.; Tatusova, T.; Lipman, D. *Gnomon-NCBI Eukaryotic Gene Prediction Tool*; National Center for Biotechnology Information: Bethesda, MD, USA, 2010.
32. Swarbreck, S.M.; Defoin-Platel, M.; Hindle, M.; Saqi, M.; Habash, D.Z. New perspectives on glutamine synthetase in grasses. *J. Exp. Bot.* **2011**, *62*, 1511–1522. [[CrossRef](#)]
33. Prinsi, B.; Espen, L. Mineral nitrogen sources differently affect root glutamine synthetase isoforms and amino acid balance among organs in maize. *BMC Plant Biol.* **2015**, *15*, 96. [[CrossRef](#)]
34. He, Y.; Wang, M.; Dukowic-Schulze, S.; Zhou, A.; Tiang, C.L.; Shilo, S.; Sidhu, G.K.; Eichten, S.; Bradbury, P.; Springer, N.M.; et al. Genomic features shaping the landscape of meiotic double-strand-break hotspots in maize. *Proc. Natl. Acad. Sci. USA* **2017**, *114*, 12231–12236. [[CrossRef](#)]
35. Luo, C.; Li, X.; Zhang, Q.; Yan, J. Single gametophyte sequencing reveals that crossover events differ between sexes in maize. *Nat. Commun.* **2019**, *10*, 785. [[CrossRef](#)] [[PubMed](#)]
36. Wang, Y.; Li, W.; Wang, L.; Yan, J.; Lu, G.; Yang, N.; Xu, J.; Wang, Y.; Gui, S.; Chen, G.; et al. Three types of genes underlying the *Gametophyte factor1* locus cause unilateral cross incompatibility in maize. *Nat. Commun.* **2022**, *13*, 4498. [[CrossRef](#)] [[PubMed](#)]
37. Boideau, F.; Richard, G.; Coriton, O.; Huteau, V.; Belser, C.; Deniot, G.; Eber, F.; Falentin, C.; Ferreira de Carvalho, J.; Gilet, M.; et al. Epigenomic and structural events preclude recombination in *Brassica napus*. *New Phytol.* **2022**, *234*, 545–559. [[CrossRef](#)] [[PubMed](#)]

38. Concepcion, J.C.T.; Kaundun, S.S.; Morris, J.A.; Hutchings, S.J.; Strom, S.A.; Lygin, A.V.; Riechers, D.E. Resistance to a nonselective 4-hydroxyphenylpyruvate dioxygenase-inhibiting herbicide via novel reduction-dehydration-glutathione conjugation in *Amaranthus tuberculatus*. *New Phytol.* **2021**, *232*, 2089–2105. [[CrossRef](#)]
39. Huang, X.X.; Zhao, S.M.; Zhang, Y.Y.; Li, Y.J.; Shen, H.N.; Li, X.; Hou, B.K. A novel UDP-glycosyltransferase 91C1 confers specific herbicide resistance through detoxification reaction in *Arabidopsis*. *Plant Physiol. Biochem.* **2021**, *159*, 226–233. [[CrossRef](#)]
40. Lv, Z.; Zhao, M.; Wang, W.; Wang, Q.; Huang, M.; Li, C.; Lian, Q.; Xia, J.; Qi, J.; Xiang, C.; et al. Changing Gly311 to an acidic amino acid in the MATE family protein DTX6 enhances *Arabidopsis* resistance to the dihydropyridine herbicides. *Mol. Plant* **2021**, *14*, 2115–2125. [[CrossRef](#)]
41. Pan, L.; Yu, Q.; Wang, J.; Han, H.; Mao, L.; Nyporko, A.; Maguza, A.; Fan, L.; Bai, L.; Powles, S. An ABCC-type transporter endowing glyphosate resistance in plants. *Proc. Natl. Acad. Sci. USA* **2021**, *118*, e2100136118. [[CrossRef](#)]
42. Xu, R.; Liu, X.; Li, J.; Qin, R.; Wei, P. Identification of herbicide resistance OsACC1 mutations via in planta prime-editing-library screening in rice. *Nat. Plants* **2021**, *7*, 888–892. [[CrossRef](#)]
43. Shen, J.; Yang, Q.; Hao, L.; Zhang, L.; Li, X.; Zheng, M. The Metabolism of a Novel Cytochrome P450 (CYP77B34) in Tribenuron-Methyl-Resistant *Descurainia sophia* L. to Herbicides with Different Mode of Actions. *Int. J. Mol. Sci.* **2022**, *23*, 5812. [[CrossRef](#)]
44. Garcia, M.D.; Nouwens, A.; Lonhienne, T.G.; Guddat, L.W. Comprehensive understanding of acetohydroxyacid synthase inhibition by different herbicide families. *Proc. Natl. Acad. Sci. USA* **2017**, *114*, E1091–E1100. [[CrossRef](#)]
45. Tian, H.; Yang, Y.; Yi, H.; Xu, L.; He, H.; Fan, Y.; Wang, L.; Ge, J.; Liu, Y.; Wang, F.; et al. New resources for genetic studies in maize (*Zea mays* L.): A genome-wide Maize6H-60K single nucleotide polymorphism array and its application. *Plant J.* **2021**, *105*, 1113–1122. [[CrossRef](#)] [[PubMed](#)]
46. da Maia, L.C.; Palmieri, D.A.; de Souza, V.Q.; Kopp, M.M.; de Carvalho, F.I.; Costa de Oliveira, A. SSR locator: Tool for simple sequence repeat discovery integrated with primer design and PCR simulation. *Int. J. Plant Genom.* **2008**, *2008*, 412696. [[CrossRef](#)] [[PubMed](#)]
47. Saghai-Marooif, M.A.; Soliman, K.M.; Jorgenson, R.A.; Allard, R.W. Ribosomal DNA spacer-length polymorphisms in barley: Mendelian inheritance, chromosomal location, and population dynamics. *Proc. Natl. Acad. Sci. USA* **1984**, *81*, 8014–8018. [[CrossRef](#)] [[PubMed](#)]
48. Altschul, S.; Gish, W.; Miller, W.; Myers, E.; Lipman, D. Basic local alignment search tool. *J. Mol. Biol.* **1990**, *215*, 403–410. [[CrossRef](#)]
49. Larkin, M.A.; Blackshields, G.; Brown, N.P.; Chenna, R.; McGettigan, P.A.; McWilliam, H.; Valentin, F.; Wallace, I.M.; Wilm, A.; Lopez, R.; et al. Clustal W and Clustal X version 2.0. *Bioinformatics* **2007**, *23*, 2947–2948. [[CrossRef](#)] [[PubMed](#)]
50. Campanella, J.J.; Bitincka, L.; Smalley, J. MatGAT: An application that generates similarity/identity matrices using protein or DNA sequences. *BMC Bioinform.* **2003**, *4*, 29. [[CrossRef](#)]
51. Wintersinger, J.A.; Wasmuth, J.D. Kablammo: An interactive, web-based BLAST results visualizer. *Bioinformatics* **2015**, *31*, 1305–1306. [[CrossRef](#)]
52. An, X.; Ma, B.; Duan, M.; Dong, Z.; Liu, R.; Yuan, D.; Hou, Q.; Wu, S.; Zhang, D.; Liu, D.; et al. Molecular regulation of *ZmMs7* required for maize male fertility and development of a dominant male-sterility system in multiple species. *Proc. Natl. Acad. Sci. USA* **2020**, *117*, 23499–23509. [[CrossRef](#)]
53. Weatherburn, M.W. Phenol hypochlorite reaction for determination of ammonia. *Anal. Chem.* **1967**, *39*, 971–974. [[CrossRef](#)]
54. Ding, F.; Hu, Q.; Wang, M.; Zhang, S. Knockout of SISBPASE suppresses carbon assimilation and alters nitrogen metabolism in tomato plants. *Int. J. Mol. Sci.* **2018**, *19*, 4046. [[CrossRef](#)]